Published in final edited form as:
Nat Genet. 2002 March ; 30(3): 335–341. doi:10.1038/ng832.

Mutations in *LGI1* cause autosomal-dominant partial epilepsy with auditory features

Sergey Kalachikov[1], **Oleg Evgrafov**[1], **Barbara Ross**[1], **Melodie Winawer**[2,5], **Christie Barker-Cummings**[2,3], **Filippo Martinelli Boneschi**[2,3], **Chang Choi**[9], **Pavel Morozov**[1], **Kamna Das**[1], **Elita Teplitskaya**[1], **Andrew Yu**[1], **Eftihia Cayanis**[1], **Graciela Penchaszadeh**[1,4,8], **Andreas H. Kottmann**[9], **Timothy A. Pedley**[5], **W. Allen Hauser**[2,3,5], **Ruth Ottman**[2,3,7], and **T. Conrad Gilliam**[1,4,6,8]

1 *Columbia Genome Center, Columbia University, 630 W 168 Street, P&S Box 16, New York, New York 10032, USA*

2 *G.H. Sergievsky Center, Columbia University, 630 W 168 Street, P&S Box 16, New York, New York 10032, USA*

3 *Department of Epidemiology, Columbia University, 630 W 168 Street, P&S Box 16, New York, New York 10032, USA*

4 *Department of Psychiatry, Columbia University, 630 W 168 Street, P&S Box 16, New York, New York 10032, USA*

5 *Department of Neurology, Columbia University, 630 W 168 Street, P&S Box 16, New York, New York 10032, USA*

6 *Department of Genetics and Development, Columbia University, 630 W 168 Street, P&S Box 16, New York, New York 10032, USA*

7 *Department of Epidemiology of Brain Disorders, New York State Psychiatric Institute, New York, New York, USA*

8 *Department of Medical Genetics, New York State Psychiatric Institute, New York, New York, USA*

9 *PsychoGenics Inc., Audubon Biomedical Science and Technology Park of Columbia University, New York, New York, USA*

Abstract

The epilepsies are a common, clinically heterogeneous group of disorders defined by recurrent unprovoked seizures[1]. Here we describe identification of the causative gene in autosomal-dominant partial epilepsy with auditory features (ADPEAF, MIM 600512), a rare form of idiopathic lateral temporal lobe epilepsy characterized by partial seizures with auditory disturbances[2,3]. We constructed a complete, 4.2-Mb physical map across the genetically implicated disease-gene region, identified 28 putative genes (Fig. 1) and resequenced all or part of 21 genes before identifying presumptive mutations in one copy of the leucine-rich, glioma-inactivated 1 gene (*LGI1*) in each of five families with ADPEAF. Previous studies have indicated that loss of both copies of *LGI1* promotes glial tumor progression. We show that the expression pattern of mouse *Lgi1* is predominantly neuronal and is consistent with the anatomic regions involved in temporal lobe epilepsy. Discovery of *LGI1* as a cause of ADPEAF suggests new avenues for research on pathogenic mechanisms of idiopathic epilepsies.

Correspondence should be addressed to R.O. (e-mail: ro6@columbia.edu).

In 1995 we mapped the ADPEAF locus to a 10-cM region on chromosome 10q24 in a single extended pedigree[2]. Linkage was subsequently reported to an overlapping interval in another large family, narrowing the minimal genetic region to approximately 3 cM, assuming the causative gene was the same[4]. Analysis of additional pedigrees confirmed the linkage but failed to narrow the region further[5–7]. To screen for disease-related mutations, we resequenced all coding-exon and bordering-intron sequences from positional candidate genes in the overlap interval in one affected individual from each of three ADPEAF pedigrees showing linkage to chromosome 10q24 (families 6610, A and B; Fig. 2)[2,7]. We then genotyped putative disease-related mutations in all available family members from the three linked pedigrees, all family members from two smaller families with ADPEAF (families C and D; Fig. 2) and 123 unrelated control individuals.

Resequencing of *LGI1* identified presumptive mutations in each of the five families with ADPEAF (Table 1 and Fig. 2). All tested affected individuals from the five families harbored a single copy of a putative disease mutation, as did all obligate carriers and individuals classified as ‘unknown’ who were found to carry the disease-linked haplotype (Fig. 2). Several unaffected individuals also carried the disease haplotype and presumptive mutation. Whether these individuals manifest subclinical signs of disease or have undergone recent changes in affection status is not yet known, but the results are consistent with our previous estimate of 71% disease-gene penetrance in family 6610 (ref. 2).

To distinguish disease-related mutations from polymorphic variants, we analyzed a panel of unrelated control individuals by resequencing the entire coding region of exon 8, all of exon 6 and all of exons 3 and 4 plus intronic sequences, each in a total of 123 control individuals. Resequencing revealed several polymorphisms (none encoding amino-acid changes), but none of the five putative mutations was detected.

Three mutations predictably altered the codon frame, leading to missense mutations and premature truncation of the Lgi1 protein, whereas one point mutation in exon 8 (family D) changed a glutamic acid residue to an alanine (Fig. 3). This amino-acid residue, as well as those extending ten residues upstream and three residues downstream, was conserved in the only identifiable, full-length *LGI1* homolog, the highly conserved mouse *Lgi1* (data not shown). One putative mutation occurred in intronic DNA, changing a single nucleotide at the third base from the acceptor intron–exon junction of exon 4 (Table 1; family B). We speculated that the alteration would either lead to aberrant splicing or, if left unspliced, encode a stop codon at amino-acid residue 118, leading to truncation of the protein (Fig. 3*c*). We carried out RT–PCR on mRNA isolated from lymphoblasts prepared from a control individual and four affected individuals from family B. PCR amplification spanning the region between exons 3 and 6 identified one normal and one aberrant band in affected individuals but not in the control sample (Fig. 4*a*). DNA sequencing of this aberrant band showed that the IVS3(–3)C→A alteration led to retention of the entire intron 3 in a portion of the *LGI1* transcript produced in individuals who carried this putative mutation (Fig. 4*b*,*c*).

Chernova *et al.*[8] were the first to describe *LGI1*, upon observing that the gene was disrupted by translocation in the T98G glioblastoma multiforme (GBM) cell line and in over one-quarter of primary tumors. *LGI1* expression is absent or significantly downregulated in many high-grade but not low-grade gliomas, suggesting a role for *LGI1* in glial tumor progression[8,9]. The functional inactivation of *LGI1* in high-grade GBM tumors provides the only evidence of the protein’s function. Assuming that *LGI1* functions primarily as a tumor progressor as opposed to a tumor suppressor, mutations in *LGI1* would predictably increase the severity or progression of glial tumors rather than increase glial tumor frequency. Although we found no clear cases of glioblastomas in these families with ADPEAF, one affected male died of a brain tumor 18 months after his diagnosis. GBM is the most common malignant tumor of the adult central

nervous system and has a median post-treatment survival of less than two years. Unfortunately, the affected individual died over 30 years ago and all records and samples have been discarded.

The genomic structure of *LGI1* and the highly conserved mouse homolog (97% amino-acid homology) were recently reported[9]; a modified representation of the human gene is depicted in Fig. 3*b*. The predicted protein structure consists of a 5′ signal peptide and three functional leucine-rich repeats (LRRs), flanked by cysteine-rich repeat sequence clusters. The carboxy terminus shows no significant homology to any known protein other than the mouse homolog and is composed of two direct tandem repeats and a possible transmembrane domain. All LRR-containing proteins seem to be involved in ligand binding or protein–protein interactions, and at least half are involved in signal transduction pathways[10,11]. The presence of four cysteine residues in each of the LRR flanking repeat sequences may indicate that *LGI1* belongs to the largest group in the LRR superfamily, the adhesive proteins and receptors[10]. It seems that *LGI1* encodes a protein consisting of an extracellular domain with LRR repeat motifs, a transmembrane segment and an intracellular segment of unknown function. The extracellular portion of Lgi1 aligns most closely with a small group of proteins including the *Drosophila* proteins slit, toll and tartan, and the mammalian *Trk* gene family, in which the LRRs are known to bind nerve growth factor and other neurotrophins[10–12].

The genes *tartan* and *slit* seem to be essential in the development of the central nervous system. The tartan protein presumably functions as a membrane-bound cell-adhesion protein, and slit as a diffusible inhibitory cue for both neuronal growth-cone guidance and neuronal migration. The *Drosophila* slit protein is produced in midline glial cells where the LRR motif is required for the directional guidance of neuronal migration[13,14]. The *Drosophila* and vertebrate *slit* genes are involved both in mechanisms of growth-cone guidance and migration of entire neurons[15]. Although there is no direct evidence of functional conservation among *LGI1* and these LRR-containing genes, the role of *slit*, and perhaps *tartan*, in neuronal cell migration and neuronal growth-cone guidance is consistent with a presumptive role for *LGI1* in both epilepsy and tumor metastasis.

In humans, *LGI1* is expressed primarily in brain (cerebellum, cortex, medulla, occipital pole, frontal lobe, temporal lobe and putamen) and muscle and at lower levels in spinal cord (data not shown)[8]. Mouse *Lgi1* was also predominantly expressed in fetal brain but not in fetal lung, liver or kidney, as detected by northern-blot analysis of whole mouse embryos on embryonic days 7, 11, 15 and 17 (data not shown).

To determine whether mouse *Lgi1* mRNA was predominantly expressed in neurons or glial cells, we carried out high-resolution, chromogenic RNA *in situ* analysis (Fig. 5). The expression pattern of *Lgi1* was predominantly neuronal and was consistent with our current understanding of the anatomic regions involved in temporal lobe epilepsy. Mouse *Lgi1* was expressed in a highly specific pattern in the neocortex and limbic regions. In the hippocampus, the amount of expression was highest in the granule cells of the dentate gyrus, the large-bodied cells within the hilus of the dentate gyrus and the pyramidal cells of the CA3 region, and much lower in the CA1 region. *Lgi1* was also expressed in the amygdala, the piriform cortex and in distinct laminae of the dorsal lateral cortex, including the auditory cortex of mice. The degree of expression of *Lgi1* varied among different brain nuclei and among individual cells within distinct brain nuclei (Fig. 5*i*), indicating a finely tuned transcriptional regulation and raising the possibility that differences in the amount of Lgi1 produced by individual cells are of functional importance.

All of the genes previously identified as causing idiopathic epilepsy syndromes in humans have been voltage-gated or ligand-gated ion channels[16], and only one gene with a different (but unknown) mechanism has been reported in a mouse model[17]. *LGI1* is not homologous to any

known ion channel gene. Although there are no direct experimental data addressing the function of *LGI1*, its homology to other genes encoding LRR-containing proteins and its presumptive role in glioma tumor progression suggest a role in cell–cell communication. It is intriguing to speculate whether LGI1 functions like slit and tartan, or other LRR-containing adhesion proteins, in neuronal-cell migration and axon growth-cone guidance in the developing central nervous system, such that loss of a single gene copy would interfere with normal neuronal development and lead to focal seizures and other symptoms of ADPEAF. Loss of both *LGI1* gene copies might lead to glial cell metastasis by upsetting neuron–glia homeostasis, perhaps through loss of neuronal inhibition of glial cell proliferation or differentiation.

We have reported five putative disease mutations in five families with ADPEAF[2,3,7]. Based on segregation patterns in affected families, predicted effects of mutations on protein sequence and lack of detection in control samples, it is likely that several, if not all, of the candidate mutations lead to temporal lobe epilepsy through haploinsufficiency. Although preliminary data indicate that loss of both copies of human *LGI1* promotes glial tumor progression, it is not clear from the current study how the homozygous loss of a predominantly neuronal gene produces this effect. Such an effect is clearly possible, however, because neurons are known to inhibit glial mitosis, and interactions between neurons and glia apparently establish precisely regulated homeostasis in both tissues.

Methods

Subjects

This study was approved by the Columbia Presbyterian Medical Center Institutional Review Board.

Since our original linkage report, we have actively sought families with ADPEAF through a variety of methods, including solicitation of referrals through a letter to the members of the American Epilepsy Society, presentations at Epilepsy Foundation meetings and a study web site. Given the distinct auditory symptoms in the original family (and the relative rarity with which they are reported), we specifically selected families for inclusion if they contained more than one individual with auditory symptoms.

We screened each subject for occurrence of seizure disorders through a telephone interview administered either directly or to a close relative. To ensure complete ascertainment of childhood seizures, we also, whenever possible, administered screening interviews to a parent. A neurologist or physician with special training in epilepsy then administered a semistructured diagnostic interview to each subject reported to have had afebrile seizures. The diagnostic interview obtained information on seizure semiology through both verbatim descriptions and structured questions about signs and symptoms, and on seizure etiology through questions about the history and timing of specific risk factors for epilepsy. We requested medical records when information from the diagnostic interview was ambiguous or further clarification was needed. We used information from the medical records on seizure histories and the results of EEGs, imaging studies and neurological examinations to supplement the information from the diagnostic interview when available.

Final diagnoses were assigned by expert neurologists (W.A.H. and T.A.P.), based on a review of all of the data collected on each subject. Epilepsy was defined as a lifetime history of two or more unprovoked seizures. We classified subjects with epilepsy who had a history of an insult to the central nervous system prior to the first unprovoked seizure as ‘remote symptomatic’ and those with no identified cause as ‘idiopathic’. Seizures precipitated by acute alterations in homeostasis or insults to the central nervous system (including febrile seizures) were excluded from the definition of epilepsy and classified as ‘acute symptomatic’. Epilepsies

were classified according to the 1989 criteria of the International League Against Epilepsy for classification of epileptic syndromes[18]. To ensure that diagnoses were made blindly with respect to those of other family members, we removed identifying information prior to consensus review and reviewed subjects from different families (including many with epilepsies other than ADPEAF) in random order.

A detailed clinical description of the families and the results of linkage analysis has been presented elsewhere[2,3,7]. Briefly, epilepsy was related to localization in all of those with idiopathic epilepsy who could be classified. Among those with idiopathic epilepsy, auditory symptoms were reported by 6 of 11 (55%) in family 6610, 4 of 4 (100%) in family A, 6 of 9 (67%) in family B, 2 of 3 (67%) in family C and 2 of 3 (67%) in family D. Other (primarily sensory) symptoms were also reported in all five families.

Genotyping and linkage analysis

We extracted DNA from blood and lymphoblastoid cell lines by established methods and generated and scored genotypes using a semi-automated high-throughput approach with fluorescently labeled microsatellite markers and ABI 377 sequencers[19].

For linkage analysis in families A, B and C, we used seven microsatellite markers: *D10S185, D10S200, D10S198, D10S603, D10S192, D10S222* and *D10S566* (ref. 7). We initially conducted a two-point parametric analysis using the ANALYZE package[20]. As in our previous analysis, we assumed an autosomal dominant model with 71% penetrance and a disease allele frequency of 0.001. We computed allele frequencies using all family members. We subsequently conducted multipoint parametric and nonparametric linkage analyses as implemented in GENEHUNTER2 (ref. 21), using the scoring function based on allele-sharing among all affected relatives simultaneously. For locus order and intermarker distance, we used the maps from the Marshfield Medical Research Foundation.

In the two-point parametric analysis the maximum lod score was 1.86 for *D10S603*, providing significant evidence for confirmation of our earlier finding. Both the multipoint parametric analysis and nonparametric analysis strengthened the findings from the two-point analysis. The strongest support for linkage was observed for *D10S603* (lod=2.93; NPL=8.06, P=0.001354). The support for linkage for adjacent markers decreased, although not substantially.

Sequence analysis

We isolated DNA samples for sequence analysis from subjects' blood or Epstein–Barr virus (EBV)–transformed lymphoblastoid cell lines. We prepared control DNAs from a panel of 123 unrelated individuals composed of one healthy married-in individual from each of 123 families collected predominantly from 13 states in the US. The majority of families were of European descent, and the families contained no known cases of epilepsy. We designed oligonucleotide PCR primers to amplify intron–exon junctions and complete exonic coding sequences. We purified PCR amplification products over 96-well glass-fiber plates (Whatman) and sequenced in both directions using dye-terminator chemistry and ABI 373 automated sequencers. We determined sequence variants using the SEQUENCHER3 program (Gene Codes Corporation) and verified by manual inspection. Because detection of heterozygous alleles is complicated by preferential PCR amplification of one allele and by context-dependent bias in dye-terminator incorporation during cycle sequencing, we limited PCR cycles to 30 and inspected all sequence traces manually. We carried out sequence analysis blind to disease status or haplotype, analyzing control samples together with known mutation carriers. In all cases, 'blind' analysis detected mutations in the known mutation carriers.

Physical mapping

We used the GeneBridge 4 radiation hybrid mapping panel (Research Genetics) and the Whitehead radiation hybrid map server to physically map the region between flanking genetic markers *D10S200* and *D10S577*. We used sequence-tagged sites and expressed sequence–tagged (EST) sequences from the radiation hybrid map as BLASTN queries against the HTGS division of the National Centre for Biotechnology Information (NCBI) GenBank database. To identify regions of overlap, we retrieved the corresponding BAC clones from this search and systematically aligned and compared them by BLAST analysis. We carried out a similar search on genomic DNA downloaded from the Celera Discovery database, which generated a series of 0.5-Mb genomic fragments spanning the region. Comparison and organization of chromosome 10q24 DNA from HTGS and Celera allowed us to compile a single uninterrupted BAC contig across the minimal genetic region.

Gene identification and modeling

We used BAC sequences and Celera genomic sequences to search EST databases for homologs. Several published maps of 10q24 greatly facilitated our efforts[22–24]. We obtained 108 Unigene EST clusters from the human GeneMap 99 web site at NCBI. In addition, we retrieved 22,500 EST sequences directly from dbEST after BLASTN searches with BAC and genomic sequences. We used in-house software to cluster these sequences into longer cDNA sequences and then aligned them with the genomic scaffold using pairwise BLASTN alignments[25]. In a few cases, we carried out RACE to extend cDNA sequences.

Reverse transcription and PCR amplification

We used RNeasy Midiprep columns (Qiagen) according to the manufacturer's suggestions to isolate total RNA from EBV-transformed lymphoblastoid cell lines. We removed DNA contamination from the total RNA samples by DNAse I treatment. We eluted total RNA from the RNeasy columns and further purified remaining poly(A)$^+$ RNA using the Oligotex kit (Qiagen). We converted poly(A)$^+$ RNA to cDNA by the process of oligo(dT)-primed reverse transcription using SuperScript II (Invitrogen/LTI). We amplified the *LGI1* cDNA segment bounded by exons 3 and 6 by an initial 35-cycle primary PCR amplification, followed by a 35-cycle nested PCR amplification. We separated the resulting fragments on 3% agarose gels and sequenced them using Big Dye Terminator chemistry (ABI).

In situ hybridization histochemistry

We generated a mouse *Lgi1* probe by PCR amplification of mouse brain cDNA. The probe consisted of an 860 bp fragment generated from the 3′ end of the mouse RNA transcript and included both coding DNA and flanking 3′ noncoding sequences. We generated oligonucleotide primers with flanking T3 and T7 RNA promoter sequences (primer sequences are available upon request).

We purified the PCR-amplified product by agarose gel electrophoresis and then used it for the synthesis of digoxigenin-labeled sense and anti-sense *in situ* hybridization probes. Coronal cryosections, 16 μm thick, of fresh frozen brains derived from 10-wk mice were hybridized with these riboprobes[26].

URLs

Transmembrane region prediction methods: http://www.hgmp.mrc.ac.uk/GenomeWeb/prot-transmembrane.html; Whitehead RH map server: http://www.genome.wi.mit.edu/cgi-bin/contig/rhmapper.

Acknowledgements

This work was supported by grants from the National Institutes of Health, National Institute of Neurological Disorders and Stroke and by funds from the Columbia Genome Center. We thank A. Efstratiadis, I. Dragatsis, I. Lipkin, M. Hornig and H. Scharfman for their critical discussions and helpful suggestions; J. Ju, A.K. Tong and C. Wang for timely technical assistance; P. McCabe, C.D. McNew and S.R. Resor for family referrals and W. Jimenez for assistance with database management. This research would not have been possible without the generous participation of the families described.

References

1. Hauser WA, Annegers JF, Kurland LT. Prevalence of epilepsy in Rochester, Minnesota: 1940–1980. Epilepsia 1991;32:429–445. [PubMed: 1868801]
2. Ottman R, et al. Localization of a gene for partial epilepsy to chromosome 10q. Nature Genet 1995;10:56–60. [PubMed: 7647791]
3. Winawer MR, Ottman R, Hauser WA, Pedley TA. Autosomal dominant partial epilepsy with auditory features: defining the phenotype. Neurology 2000;54:2173–2176. [PubMed: 10851389]
4. Poza JJ, et al. Autosomal dominant lateral temporal epilepsy: clinical and genetic study of a large Basque pedigree linked to chromosome 10q. Ann Neurol 1999;45:182–188. [PubMed: 9989620]
5. Michelucci R, et al. Autosomal dominant partial epilepsy with auditory features: description of a new family. Epilepsia 2000;41:967–970. [PubMed: 10961622]
6. Mautner VF, Lindenau M, Gottesleben A, Goetze G, Kluwe L. Supporting evidence of a gene for partial epilepsy on 10q. Neurogenetics 2000;3:31–34. [PubMed: 11085594]
7. Winawer MR, et al. Four new families with autosomal dominant partial epilepsy with auditory features: clinical description and linkage to chromosome 10q24. Epilepsia 2002;43:55–66.
8. Chernova OB, Somerville RP, Cowell JK. A novel gene, *LGI1*, from 10q24 is rearranged and downregulated in malignant brain tumors. Oncogene 1998;17:2873–2881. [PubMed: 9879993]
9. Somerville RP, Chernova O, Liu S, Shoshan Y, Cowell JK. Identification of the promoter, genomic structure, and mouse ortholog of *LGI1*. Mamm Genome 2000;11:622–627. [PubMed: 10920229]
10. Kobe B, Deisenhofer J. The leucine-rich repeat: a versatile binding motif. Trends Biochem Sci 1994;19:415–421. [PubMed: 7817399]
11. Kobe B, Deisenhofer J. Proteins with leucine-rich repeats. Curr Opin Struct Biol 1995;5:409–416. [PubMed: 7583641]
12. Chang Z, et al. Molecular and genetic characterization of the *Drosophila tartan* gene. Dev Biol 1993;160:315–332. [PubMed: 8253267]
13. Battye R, Stevens A, Perry RL, Jacobs JR. Repellent signaling by Slit requires the leucine-rich repeats. J Neurosci 2001;21:4290–4298. [PubMed: 11404414]
14. Wu W, et al. Directional guidance of neuronal migration in the olfactory system by the protein Slit. Nature 1999;400:331–336. [PubMed: 10432110]
15. Kidd T, Bland KS, Goodman CS. Slit is the midline repellent for the robo receptor in *Drosophila*. Cell 1999;96:785–794. [PubMed: 10102267]
16. Meisler MH, Kearney J, Ottman R, Escayg A. Identification of epilepsy genes in human and mouse. Annu Rev Genet 2001;35:567–588. [PubMed: 11700294]
17. Skradski SL, et al. A novel gene causing a mendelian audiogenic mouse epilepsy. Neuron 2001;31:537–544. [PubMed: 11545713]
18. Commission on Classification, Terminology ILAE. Proposal for revised classification of epilepsies and epileptic syndromes. Epilepsia 1989;30:389–399. [PubMed: 2502382]
19. Aita VM, et al. A comprehensive linkage analysis of chromosome 21q22 supports prior evidence for a putative bipolar affective disorder locus. Am J Hum Genet 1999;64:210–217. [PubMed: 9915960]
20. Goring HH, Terwilliger JD. Linkage analysis in the presence of errors. III: Marker loci and their map as nuisance parameters. Am J Hum Genet 2000;66:1298–1309. [PubMed: 10731467]
21. Kruglyak L, Daly MJ, Reeve-Daly MP, Lander ES. Parametric and nonparametric linkage analysis: a unified multipoint approach. Am J Hum Genet 1996;58:1347–1363. [PubMed: 8651312]

22. Gray IC, Nobile C, Muresu R, Ford S, Spurr NK. A 2.4-megabase physical map spanning the CYP2C gene cluster on chromosome 10q24. Genomics 1995;28:328–332. [PubMed: 8530044]

23. Gray IC, et al. An integrated physical and genetic map spanning chromosome band 10q24. Genomics 1997;43:85–88. [PubMed: 9226376]

24. Nobile C, et al. A refined physical and EST map spanning 7.4 Mb of 10q24, a region involved in neurological disorders. Mamm Genome 1998;9:835–837. [PubMed: 9745040]

25. Tatusova TA, Madden TL. BLAST 2 Sequences, a new tool for comparing protein and nucleotide sequences. FEMS Microbiol Lett 1999;174:247–250. [PubMed: 10339815]

26. Schaeren-Wiemers N, Gerfin-Moser A. A single protocol to detect transcripts of various types and expression levels in neural tissue and cultured cells: *in situ* hybridization using digoxigenin-labelled cRNA probes. Histochemistry 1993;100:431–440. [PubMed: 7512949]

27. Engelman DM, Steitz TA, Goldman A. Identifying nonpolar transbilayer helices in amino acid sequences of membrane proteins. Annu Rev Biophys Biophys Chem 1986;15:321–353. [PubMed: 3521657]

28. Juretic D, Zucic D, Lucic B, Trinajstic N. Preference functions for prediction of membrane-buried helices in integral membrane proteins. Comput Chem 1998;22:279–294. [PubMed: 9680689]

29. Milpetz F, Argos P, Persson B. TMAP: a new email and WWW service for membrane-protein structural predictions. Trends Biochem Sci 1995;20:204–205. [PubMed: 7610486]

30. Shah AB, et al. Identification and analysis of mutations in the Wilson disease gene (ATP7B): population frequencies, genotype–phenotype correlation, and functional analyses. Am J Hum Genet 1997;61:317–328. [PubMed: 9311736]

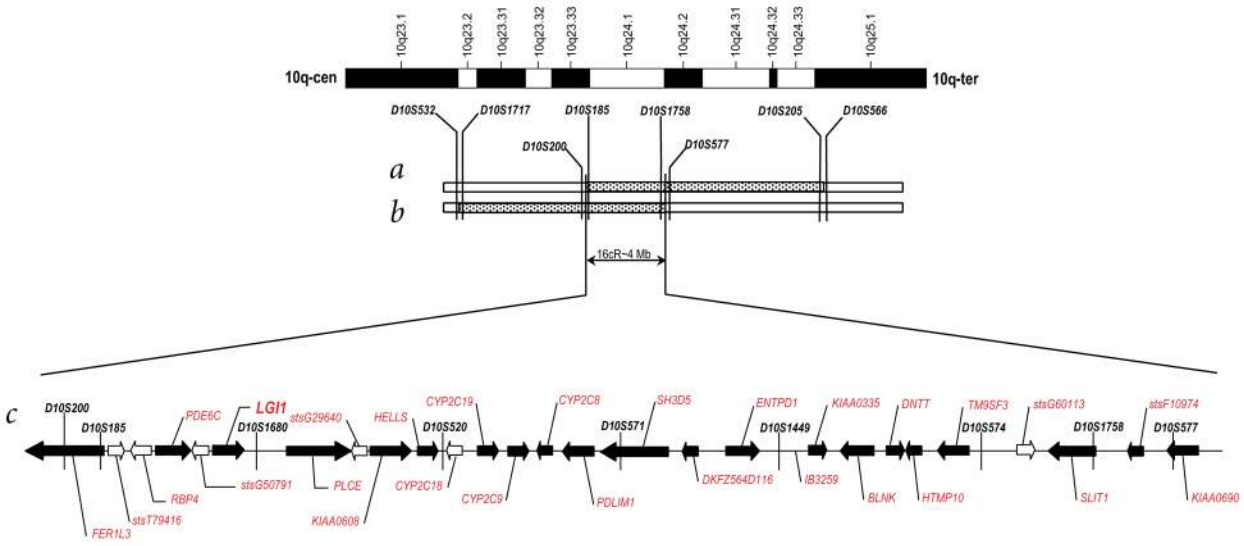

Fig. 1.

Transcript map of the genetically defined interval for ADPEAF on chromosome 10q24. The minimal genetic region believed to harbor the ADPEAF gene is shown. ***a***,***b***, The speckled bars denote minimal genetic regions defined by the linkage studies of Ottman *et al.*[2] (*a*; top bar) and Poza *et al.*[4] (*b*; bottom bar). The 3-cM region of overlap was flanked by locus *D10S200* on the centromeric boundary and by *D10S577* at the telomeric boundary. Radiation hybrid mapping analysis predicted that the interval would span 16 cR, which corresponds to 4 Mb on human chromosome 10. Physical mapping further refined the region to 4.2 Mb. ***c***, A transcript map of the region constructed by combining data from Human Gene Map 99 from NCBI with basic local alignment search tool predictions generated by comparison of 10q24 genomic DNA with the dbEST database. A total of 47 independent ESTs were identified, 28 of which contained unambiguous ORFs. These putative genes are listed in red, and microsatellite markers in black. Arrows indicate the direction of transcription. Black arrows indicate that the candidate gene was screened for ADPEAF-related mutations. *SLIT1*, a gene with a gene structure and expression similar to that of *LGI1*, is located in the interval approximately 3.2 Mb telomeric to *LGI1*.

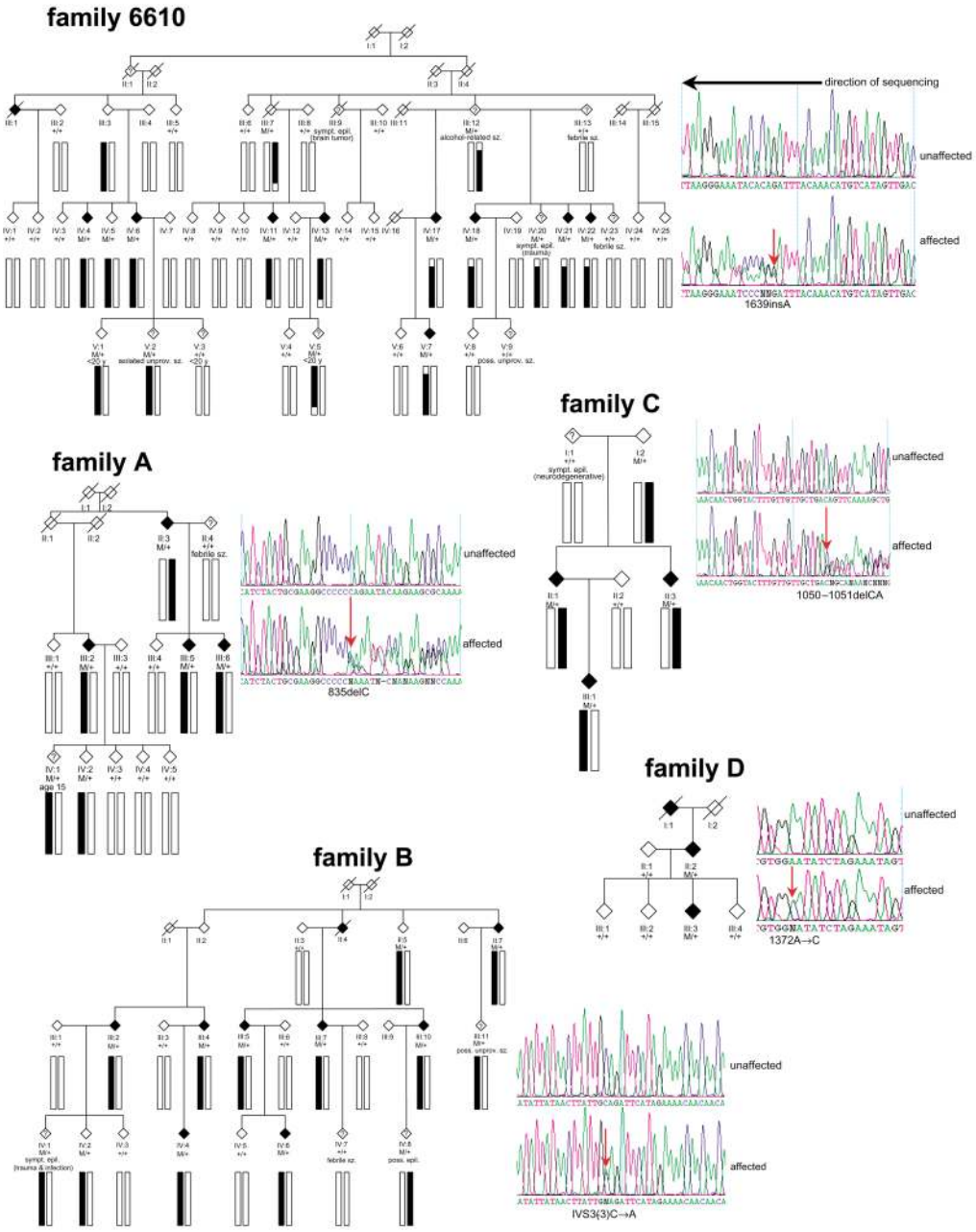

Fig. 2.

Segregation of putative disease alleles in families with ADPEAF. Family 6610 is the original family used to establish linkage between 10q24 DNA markers and disease[2]. Filled bars mark the presence and boundaries of disease-related haplotypes, defined in families A, B and C by markers *D10S185, D10S200, D10S198, D10S603, D10S192, D10S222* and *D10S566*, and in family 6610 by these markers excluding *D10S192*. The markers span a sex-averaged distance of 10.8 cM, according to the Marshfield map. Individuals who did not carry mutations are denoted by +/+, and those who carried one mutant and one normal allele by M/+. Original sequence tracings used to detect putative disease alleles are shown to the right of each family pedigree. Variant alleles are denoted by red arrows. Families 6610, A and B had insertion or deletion mutations, and the sequence traces show ‘signatures’ characteristic of heterozygous

changes by which the diploid sequences became asynchronous, beginning with the mutant nucleotide. To be certain of the actual mutation, *LGI1* DNA was subcloned and sequenced as haploid DNA from each of the families, and haploid cell lines were derived for family 6610 (GMP Companies; data not shown). Filled symbols represent individuals with idiopathic epilepsy; symbols containing a '?' represent individuals classified as 'unknown', either because they had symptomatic epilepsy (sympt. epil.), febrile seizures (febrile sz.), alcohol-related acute symptomatic seizures (alcohol-related sz.) or isolated unprovoked seizure (isol. unprov. sz.), because they were under 20 y at the time of clinical assessment or because their final diagnosis was 'possible' (rather than definite) epilepsy (poss. epil.). A detailed clinical description of each family has been presented separately[2,3,7].

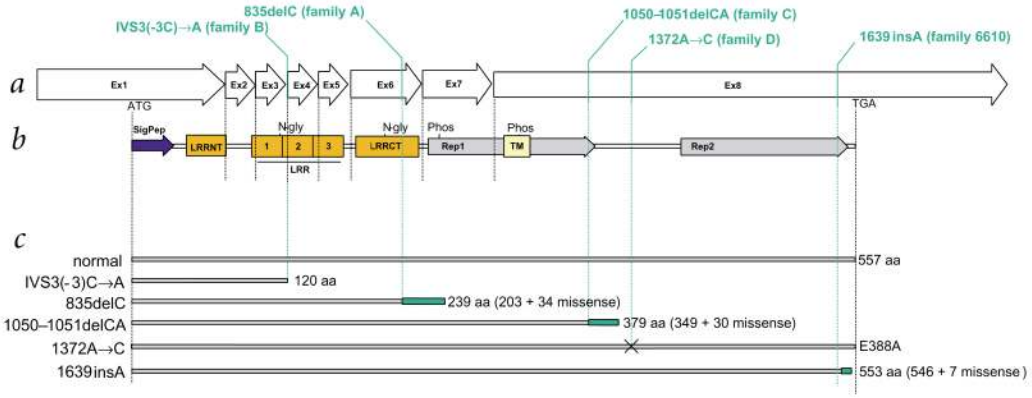

Fig. 3.

Predicted effect of ADPEAF mutations on Lgi1. ***a***, Structural organization of *LGI1*. *LGI1* spans 36.9 kb and consists of eight exons ranging in size from 72 bp (exons 2–5) to 1,197 bp (exon 8). The mRNA transcript consists of a 262-bp 3′ UTR and a 1,674-bp ORF[8]. Exon 1 includes a signal peptide, and exons 3–5 each contain a full 24-aa LRR motif (spanning from the fifth amino acid of one repeat to the fifth amino acid of the next). Putative mutations are illustrated by their corresponding family identifiers. Three were located in exon 8, one in exon 6 and one (from family B) in the 95-bp intron between exons 3 and 4. ***b***, Predicted sequence motifs in Lgi1. This figure is a modification of those previously presented[8,9]. Beginning at the amino terminus (left), the protein contained a predicted signal peptide (filled arrow; positions 1–35), an N-terminal cysteine-rich LRR flanking sequence (LRRNT; residues 45–71), three LRR repeat sequences (orange boxes; residues 90–113, 114–137 and 138–161), a C-terminal cysteine-rich LRR flanking sequence (LRRCT; residues 173–222), two direct repeat sequences (Rep1 and 2; residues 226–361 and 420–549, respectively) and a putative membrane-spanning segment (yellow rectangle). A 22-bp transmembrane region (residues 288–309) was previously reported[9]. We found support for this prediction using several methods[27], including the dense alignment surface (DAS) method for predicting integral membrane proteins[28,29], although other methods (PRED-TMR) fail to predict the region. A fourth putative LRR repeat, predicted by Sommerville *et al.*[9], resided N-terminally to the other three repeats and was encoded by exon 2. Although it seemed to share a common origin with the other repeats, its divergence at canonical residues made its role as a functional LRR repeat ambiguous. Chernova *et al.*[8] predicted two potential N-glycosylation sites at Asn192 and Asn277 and potential phosphorylation sites for cAMP-dependent protein kinase (Ser 313), tyrosine kinase (Tyr 384) and several sites for PKC and casein kinase II. Lgi1 is predicted to consist of 557 amino-acid residues and to encode a slightly alkaline 60-kD protein (after removal of the signal peptide). ***c***, Predicted effect of mutations on protein sequence. The predicted effect of each of the five presumptive ADPEAF mutations is depicted relative to the ‘normal’ protein shown to encode 557 amino-acid residues. The single–base pair insertion in family 6610 would predictably encode an Lgi1 protein with a normal complement of the first N-terminal 546 amino acids, followed by seven missense residues and four truncated residues. The Lgi1 extracellular region and the C-terminal region were highly conserved between human and mouse. Likewise, the frameshift mutations in families A and C would predictably alter protein structure and function dramatically. Family B showed a C→A transversion at position −3′ relative to the exon 4 acceptor splice site. Whereas positions −1 and −2 are typically conserved and often lead to cryptic site usage or exon skipping when altered[30], little is known about the effects of alteration at the −3 position. The presumptive mutation led to retention of intron 3 in a portion of *LGI1* transcripts from affected individuals (Fig. 4). Family D showed a non-conservative missense mutation in exon 8.

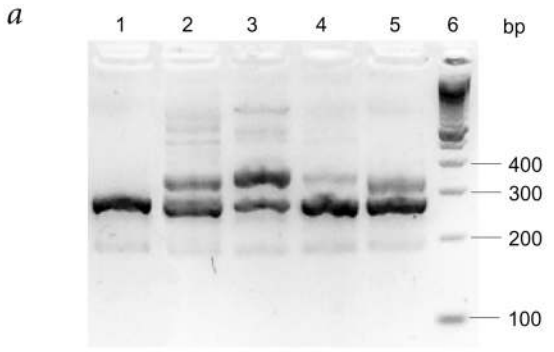

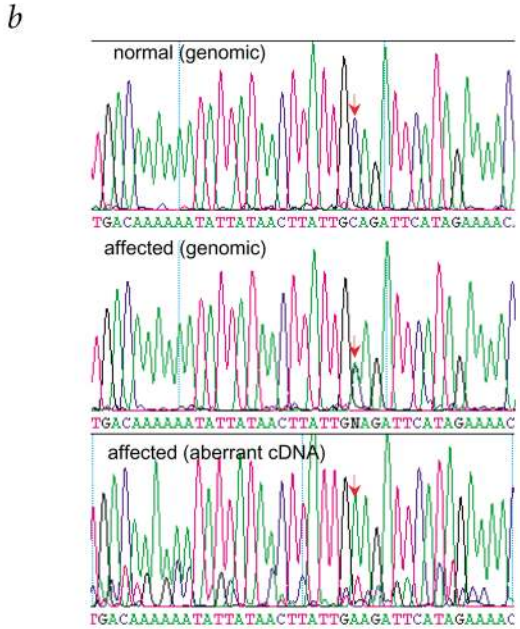

Fig. 4.

Aberrant *LGI1* splicing in family B. ***a***, *LGI1* oligonucleotide primers specific for exon 3 and exon 6 were amplified using RT–PCR and mRNA isolated from lymphoblastoid cell lines. Lane 1, control sample; lanes 2–5, samples from four affected individuals in family B; lane 6, 100-bp size standards. All sample lanes showed a 286-bp fragment corresponding to the normal transcript. Samples from affected individuals also showed a second band that included a 72-bp insertion corresponding to the intact intron 3. ***b***, Alignment of DNA sequencing traces corresponding to genomic DNA from a control individual (top panel) and an individual from family B with epilepsy (middle panel), together with the sequence trace corresponding to the aberrant RT–PCR fragment (bottom panel) derived from the same cell line represented in the middle panel. As expected, the genomic trace from the individual with epilepsy showed a C/

A heterozygote at IVS3(–3), whereas the aberrant RT–PCR fragment contained exclusively adenine at the same position. ***c***, Sequence alignment of the aberrant (top) and normal (bottom) *LGI1* amplification fragments. A complete copy of intron 3 was retained in the aberrant transcript, introducing a putative stop codon (blue type) at the start of intron 3. The presumptive splice-site mutation is shown in red.

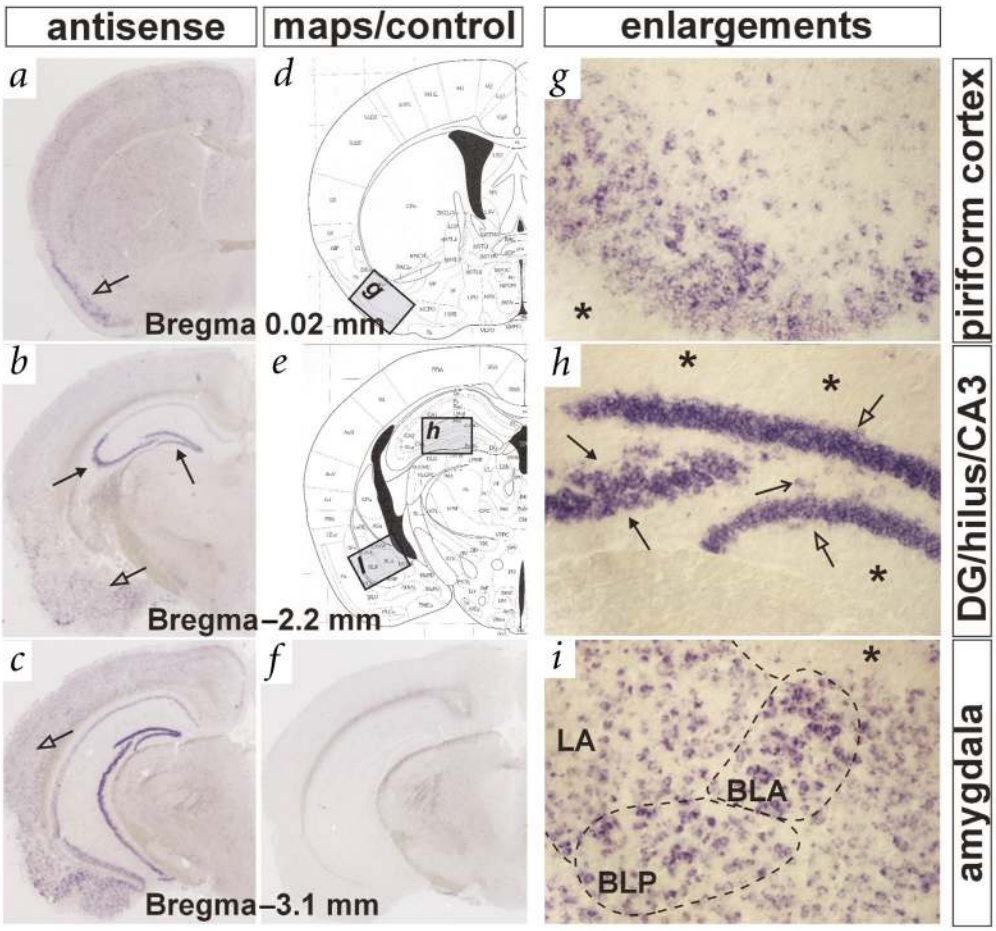

Fig. 5.

Analysis of *Lgi1* expression in the adult mouse brain by chromogenic RNA *in situ* hybridization. ***a–c,f***, An antisense riboprobe (*a–c*) or a sense (control) riboprobe (*f*) of *Lgi1* was hybridized to 16-μm thin coronal cryosections of brains harvested from 10-wk mice (see Methods). Shown are representative sections from the anterior to the posterior extent of the temporal cortex (×40). Bregma values refer to the classical coordinates for vertebrate sections along the anterior–posterior axis. In *a*, the arrow marks the piriform cortex; in *b*, the open arrow marks the amygdala and the closed arrows the CA3 region and the dentate gyrus of the hippocampal formation. In *c*, the arrow marks the location of the mouse auditory cortex. As seen in the low-power images of *a–c*, *Lgi1* was expressed more in ventral cortical structures than dorsal structures. Careful inspection of these sections, however, revealed *Lgi1*-expressing cells in distinct areas of the dorsal cortex. ***d,e***, Brain maps of the piriform cortex (*d*) and the dentate gyrus and amygdala (*e*). ***g–i***, Enlargements of *Lgi1* expression in the piriform cortex, dentate gyrus and amygdala, respectively (×200). The relative location of each of these brain regions is identified by rectangular boxes on the brain maps depicted in *d* and *e*. Stars in *g–i* denote molecular areas or fiber tracts that seemed to be generally devoid of *Lgi1*-expressing cells, whereas areas that were densely packed with neurons demonstrated high *Lgi1* expression (arrows in *g–i*). This restricted expression of *Lgi1* was especially apparent in the hippocampal formation (*h*). Here *Lgi1* expression was constrained to the granular cells of the dentate gyrus (closed arrows), to large-bodied cells within the hilus of the dentate gyrus (open arrows) and to the pyramidal cells of the CA3 region (solid arrows) but was absent from the molecular areas (stars in *h*). The *in situ* analysis also revealed the presence of distinct mRNA levels in individual

cells in both the piriform cortex (*g*) and amygdala (*i*). Cells within the basolateral nuclei of the amygdala (BLP, basolateral amygdala posterior; BLA, basolateral amygdala anterior) seemed to express distinctly larger amounts of *Lgi1* than did cells within the lateral nuclei of the amygdala (LA in *i*).

Table 1

LGI1 mutations in families with ADPEAF

Family	Exon	Mutation[a]	Predicted result
6610	8	1639insA	frameshift, protein truncation
A	6	835delC	frameshift, protein truncation
B	3–4	IVS3(–3)C→A	intron retention, protein truncation
C	8	1050–1051delCA	frameshift, protein truncation
D	8	1372A→C	Glu383Ala

[a]Mutations are named according to recommendations of the Nomenclature System for Human Gene Mutations. The Gen-Bank mRNA sequence (NM_005097) of *LGI1* is used as a reference. The A of ATG of the initiator codon is denoted as +1.